Study on the Sparse Sub-block Microwave Imaging Based on Lasso

Xiang Yin* Zhang Bing-chen Hong Wen

(*Institute of Electronics*, *Chinese Academy of Sciences*, *Beijing* 100190, *China*)

Abstract: Sparse microwave imaging requires a nonlinear algorithm that is expensive for large scene imaging. Therefore, the sub-block imaging method, in which the measured data and the relative imaging region are divided into sub-blocks, is studied. Then, a sparse microwave imaging algorithm based on the Least absolute shrinkage and selection operator (Lasso) is performed on each sub-block. Finally, the sub-blocks are combined to obtain the whole image of the large scene. When compared with the overall reconstruction of the sparse scene, the sub-block algorithm can control the amount of data involved in each reconstruction, thereby avoiding frequent accessing of the disk by the signal processor, which is time consuming. Further, the theoretical analysis illustrates that the sub-block sparse imaging method is also accurate and stable, and the associated reconstruction error is no more than two times that of the overall reconstruction. The simulation and real data processing results support the validity of our method.

Key words: Microwave imaging; Sparse signal processing; Sparse microwave imaging; Least absolute shrinkage and selection operator (Lasso); Sub-block imaging

CLC index: TN958

DOI: 10.3724/SP.J.1300.2013.13011

基于 Lasso 的稀疏微波成像分块成像原理与方法研究

向 寅 张冰尘 洪 文

(中国科学院电子学研究所 北京 100190)

摘 要：稀疏微波成像需要使用相对复杂的非线性处理方法，这些方法难于处理大场景成像问题，为此，该文提出了一种适用于大场景稀疏微波成像的分块成像方法。该方法首先将大场景观测数据和成像区域分割成一一对应的子数据块和子区域，然后利用基于 Lasso 的稀疏微波成像方法对各子区域独立重建，最后拼接子区域重建结果得到大场景整体图像。相比于对稀疏观测场景进行整体重建，该分块处理方法可以控制每次重建所涉及的数据量，同时理论分析表明分块处理稀疏场景重建误差不超过整体重建误差上界的两倍。数值仿真及实测数据处理结果验证了该分块处理方法的有效性。

关键词：微波成像；稀疏信号处理；稀疏微波成像；Lasso；分块成像

中图分类号：TN958 **文献标识码**：A **文章编号**：2095-283X(2013)03-0271-07

1 Introduction

The microwave imaging is a coherent imaging technology that aims to observe the target of interest on land, in ocean, sky or the outer space and can work in all daylong and all-weather conditions. It is widely used in national defense and warning, marine monitoring, topography, agriculture and disaster monitoring[1]. Modern microwave imaging technology requires higher resolution and wider swath, so that the hardware level and the inherent imaging system have become the bottleneck of the development of the microwave imaging. By transforming imaging problem into reconstruction of sparse signal, sparse signal processing can significantly reduce the amount of data required when observing a specific scene, and decrease the system complexity at the same time. It has opened up the situation for innovation of the microwave imaging system and method[2].

Manuscript received February 19, 2013; revised May 29, 2013. Published online July 02, 2013.

Supported by the National Research Program of China (No. 2010CB731905).

*Corresponding author: Xiang Yin.
E-mail: xy_overlimit@sina.cn.

The researchers of sparse signal processing study on how to compress, acquire and reconstruct the sparse or compressed signal with high efficiency. From 2004, Donoho and Candès *et al.* developed the theorem of compressive sensing, which could be seemed as the greatest milestone of the sparse signal processing. It states that a high dimensional signal, sparse or compressed, can be accurately approached by means of low dimensional linear observation and nonlinear optimization methods[3,4]. Baraniuk is the first one that applies compressive sensing to radar imaging, and realizes reconstruct-tion 1-D and 2-D compressed scene form sub-Nyquist's samplers from simulation[5]. Patel starts the research that combines compressive sensing and the Synthetic Aperture Radar (SAR), and gets a focused 2-D SAR image of a car form random selected azimuth samplers[6]. In Ref. [7], Fang proposes a 2-D decoupling sparse imaging method that realizes efficient large scale SAR imaging. Other related works are concluded in the survey paper[2].

Due to the complexity of the nonlinear signal reconstructing method, the sparse signal processing is not suit for solving large or even huge scale problem, for example, the SAR imaging problem. In Ref. [6], Patel only applies sparse signal process-sing method to focus the azimuth data in each range gate, so as to avoid directly solving large scale 2-D SAR problem. In the Ref. [7], Fang has realized 2-D sparse imaging properly, but only suit for local 2-D scene which is relatively small. This method has a deficiency of repeatedly loading primitive data from hard disk to the memory of the processor, which will cost plenty of processing time.

If we can decompose the problem of non-linear large-scene sparse-imaging to several small-scene imaging problem by referring to the traditional coherent imaging technology, it will be helpful for overcoming the shortcomings talked above. Based on this consideration, this paper starts from the basic sparse signal processing frame—Least absolute shrinkage and selection operator (Lasso), studies the sparse sub-block microwave imaging of large scene. The whole paper is focused on the simple 1-D sparse scene reconstruction problem, specifics as follows:

In Section 2, we introduce a 1-D sparse scene reconstruction model and the Lasso processing method. In Section 3, we create a sub-block imaging procedure, and then discuss the stability of sub-block method by analyzing the reconstruction accuracy of sub-problem. In Section 4, this method is verified via numerical simulation and measured data by RadarSat-1. In the last, we summarize the whole paper.

2 One Dimensional Sparse Scene Reconstruction Based on Lasso

2.1 Problem of 1-D sparse scene reconstruction

Sparse scene means it contains only a few dominate scattering points and can be accurately reconstructed from low average rate observation of the echo[5]. The echo of radar is given by

$$s(t)=\int h(t-\tau)x(\tau)\mathrm{d}\tau+n(t) \tag{1}$$

where, $x(\tau)=\sum_{k=1}^{K}x_k\delta(\tau-\tau_k)$, x_k,τ_k stands for the strength and the delay of each scattering center, respectively, $h(t)$ is the radar waveform, $s(t)$ is the echo of the scene, and $n(t)$ stands for the measurement noise.

Let $\boldsymbol{y}=\boldsymbol{\Theta}\circ s=\left[s(t_1),\cdots,s(t_M)\right]^{\mathrm{T}}$ be a set of sub-samples of $s(t)$ with an average sampling rate lower than the Nyquist's rate, where $\boldsymbol{\Theta}$ stands for the linear operator of sub-sampling, and $t_1,\cdots,t_M$ is the associate sampling time. Then from Eq. (1) it gives

$$y_m=\int h(t_m-\tau)x(\tau)\mathrm{d}\tau+n(t_m),\ m=1,\cdots,M \tag{2}$$

To solve x from Eq. (2) with sparse signal processing method, $x(\tau)$ need to be decreted into a vector composed of uniform range cells: $\boldsymbol{x}=\left[\cdots,x(n\Delta\tau),\cdots\right]$, $n=1,\cdots,N$. According to the theoretical analysis of the resolution of sparse scene reconstruction[8], we choose unit size $\Delta\tau$ as radar's range resolution to maintain the stability of reconstruction. Thus, we can rewrite Eq. (2) to linear equations as:

$$\boldsymbol{y}=\boldsymbol{\Theta}\boldsymbol{H}\boldsymbol{x}+\boldsymbol{n}=\boldsymbol{\Phi}\boldsymbol{x}+\boldsymbol{n} \tag{3}$$

where $\boldsymbol{\Phi}=\boldsymbol{\Theta}\boldsymbol{H}$ is the observation matrix of the sparse microwave imaging system, which is combined by radar's observation $\boldsymbol{H}$ and the rule of sampling $\boldsymbol{\Theta}$.

2.2 The sparse signal reconstruction method based on Lasso

Lasso is a special name for L1-regularized least square method given by mathematical statistician, which can be described as

$$\hat{\boldsymbol{x}} = \arg_{\boldsymbol{x}} \min L(\boldsymbol{x});\ L(\boldsymbol{x}) = \frac{1}{2}\|\boldsymbol{y} - \boldsymbol{\Phi}\boldsymbol{x}\|_2^2 + \gamma\|\boldsymbol{x}\|_1 \quad (4)$$

where, $\| \|_2$, $\| \|_1$ is the L2-norm and the L1-norm of a vector, $\gamma > 0$ is L1-regularized constant. From the perspective of Bayesian estimation theory, Eq. (4) can be seen as a Laplace distribution with the assumption that $\boldsymbol{x}$ follows a zero-mean-value priori distribution. As the regularization reinforces (γ increases), Lasso forces more and more elements of solved value $\hat{\boldsymbol{x}}$ become zero, so Lasso is often used to solve sparse problem. Ref. [9] discussed the mathematical properties of Lasso in detail. We can draw a conclusion form Lemma 3 in Ref. [9] that on the joint supported domain $\boldsymbol{x}, \hat{\boldsymbol{x}}$, $\Lambda = \mathrm{supp}(\boldsymbol{x}) \cup \mathrm{supp}(\hat{\boldsymbol{x}})$ of $\boldsymbol{x}, \hat{\boldsymbol{x}}$, the difference between $\boldsymbol{x}$ and $\hat{\boldsymbol{x}}$ equals:

$$\boldsymbol{e}_{\boldsymbol{x},\hat{\boldsymbol{x}}} := \hat{\boldsymbol{x}}_\Lambda - \boldsymbol{x}_\Lambda = \left(\boldsymbol{\Phi}_\Lambda^* \boldsymbol{\Phi}_\Lambda\right)^{-1} \boldsymbol{\Phi}_\Lambda^* \boldsymbol{n} - \gamma \left(\boldsymbol{\Phi}_\Lambda^* \boldsymbol{\Phi}_\Lambda\right)^{-1} \boldsymbol{g} \quad (5)$$

where $\boldsymbol{\Phi}_\Lambda$ is the local observation matrix consists of indexed sequences of Λ, superscript * denotes the conjugate transpose of the matrix,

$$\boldsymbol{g}[i] = \begin{cases} \mathrm{sgn}(\hat{\boldsymbol{x}}[i]), & i \in \mathrm{supp}(\hat{\boldsymbol{x}}) \\ c[i], |c[i]| \le 1, & \text{else} \end{cases}$$

$[i]$ stands for the i-th element of the vector.

In this equation, $\boldsymbol{n}, \boldsymbol{g}$ can be seen as a random vector composed of the noise and the symbol $\hat{\boldsymbol{x}}$, thus, the variance of $\boldsymbol{e}_{\boldsymbol{x},\hat{\boldsymbol{x}}}$ mainly depends on the variance of $\boldsymbol{n}$, the value of γ and the minimum singular value of $\boldsymbol{\Phi}_\Lambda$. The smaller the variance of $\boldsymbol{e}_{\boldsymbol{x},\hat{\boldsymbol{x}}}$ is, the more likely we can accurately solve this problem.

In Eq. (5), $\boldsymbol{n}$ is independent of the signal processing method, and γ can be seen as a threshold to eliminate the noise out of $\mathrm{supp}(\hat{\boldsymbol{x}})$, which follows $\gamma \propto \boldsymbol{\Phi}^* \boldsymbol{n}$ [8]. Thus, by referring to Eq. (5), we can get:

$$\boldsymbol{e}_{\boldsymbol{x},\hat{\boldsymbol{x}}} = C\left(\boldsymbol{\Phi}_\Lambda^* \boldsymbol{\Phi}_\Lambda\right)^{-1} \boldsymbol{\Phi}_\Lambda^* \boldsymbol{n} \quad (6)$$

where C is a constant determined by the sparsity, also means the number of non-zero elements in the reconstruction vector. Eq. (6) is our starting point to study the accuracy of sparse signal reconstruction based on Lasso, in which, we know if the minimum singular value of $\boldsymbol{\Phi}_\Lambda$ is a little too small, which means $\boldsymbol{\Phi}_\Lambda^* \boldsymbol{\Phi}_\Lambda$ may not be reversible, the effect of enlarge $\boldsymbol{e}_{\boldsymbol{x},\hat{\boldsymbol{x}}}$ is obvious. So when we design the observation matrix $\boldsymbol{\Phi}$, we should guarantee the local sparse matrix of $\boldsymbol{\Phi}$, for instance, $\boldsymbol{\Phi}_\Lambda$, close to the orthogonal matrix. This is not only the requirement of Lasso, but also a universal request in sparse signal processing theory[10].

3 The Principle of Sparse Sub-block Imaging

3.1 Decompose the original problem into sub-problems

Generally speaking, non-linear problem can not be separated to several independent sub-problems to be solved. But problem Eq. (3) has its particularity. Let T be the duration of $h(t)$, when the receiving time of the constrainted echo $t \in [t_1, t_2]$, Eq. (1) can be rewritten as:

$$s(t) = \int_{t_1 - T/2}^{t_2 + T/2} h(t-\tau)x(\tau)\mathrm{d}\tau + N(t),\ t \in [t_1, t_2] \quad (7)$$

that is, targets whose echo delay time $\tau \in [t_1 - T/2, t_2 + T/2]$ will not affect this segment of echo, further more, it will not affect the down-sampled data $\{s(t_i): t_i \in [t_1, t_2],\ i = 1, \cdots\}$, which is derived by this segment of echo. Thus, compared to Eq. (1), Eq. (7) constitutes a set of independent linear sub-problems.

Fig. 1 depicts the model of the imaging sub-problem, in which, left of the picture is the sparse sample data $\boldsymbol{y}_I$ extracted from the sub-segment of echo; the parallelogram describes the distribution of non-zero elements in $\boldsymbol{H}_I$, the radar sub-matrix, and the back-scattered coefficient $\boldsymbol{x}_I$ is showed in

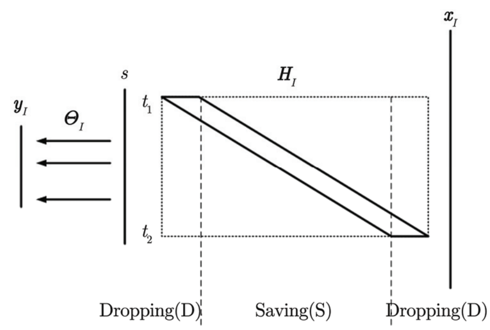

Fig. 1 Measurement model of sub-problem I

the right of the picture. This model can be expressed by mathematical formula as:

$$\boldsymbol{y}_I = \boldsymbol{\Theta}_I \boldsymbol{H}_I \boldsymbol{x}_I + \boldsymbol{n}_I = \boldsymbol{\Phi}_I \cdot \boldsymbol{x}_I + \boldsymbol{n}_I,\ I = 1, \cdots \quad (8)$$

where $\boldsymbol{\Theta}_I$ is the sparse sample matrix belongs to the I-th segment of echo, sparse signal processing method is also used when we are reconstructing $\boldsymbol{x}_I$. Formally, sub-problem Eq. (8) is the same as the integral problem model Eq. (3), but essentially, when solving the sub-problem, parts of the ultimate result should be reserved and parts should be discarded. Here, we use the definition of "area of saving" and "area of dropping" defined in the matched filtering theory: "area of saving" is the region in which the transmitted pulses completely go through and is accumulated completely. "area of dropping" is the region in which the transmitted pulses incompletely go through and is accumulated incompletely. See Fig. 1.

Fig. 2 is the reconstruction result of sparse sampled point target scene. The sample rate is 25% of the Nyquist's sample rate. Picture shows that the inequality of the response in the "area of saving" and the "area of dropping" for the responses of the same kind target. The main reason is that the contribution of the target in the "area of dropping" to the observed data is far more less than that in the "area of saving". In this case, reconstruction result in the "area of dropping" should be discarded. Indeed, because of the non-linear feature of the sparse signal processing method, these discarded result cannot be retrieved by "overlap-add" method.

Due to the discard of the reconstruction result of the "area of dropping", improper sub-problem division can cause seam when we splice the result

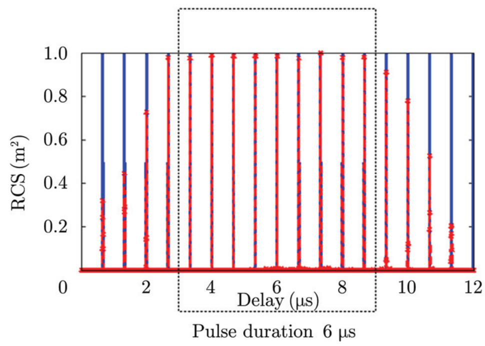

Fig. 2 Reconstruction result of Lasso (pulse duration 6 μs, bandwidth 150 MHz, 25% sub-sampling)

together. Therefore, to realize "seamless-splice", the overlap of the sampled time region of the adjacent sub-problems should be at least one pulse duration time (T).

3.2 Analysis of the sub-problem reconstruction accuracy

When we are solving the integral problem, if the design of the sample is reasonable and the scene is sufficiently sparse, then the reversible feature of the sparse regions of the observed matrix $\boldsymbol{\Phi}$ can be guaranteed. Now, calculated by Eq. (6), the Lasso sparse signal reconstruction error should be stable relative to the noise.

When we are solving the sub-problem, the division of the observed data destroy the reversible feature of some regions of $\boldsymbol{\Phi}$. Let Λ_I be $\Lambda_I = \operatorname{supp}(\boldsymbol{x}_I) \cup \operatorname{supp}(\hat{\boldsymbol{x}}_I)$, the intersection between Λ_I and area of dropping is D, the intersection between Λ_I and area of saving is S. Correspondently, denote $\boldsymbol{x}_D, \hat{\boldsymbol{x}}_D; \boldsymbol{\Phi}_D$ and $\boldsymbol{x}_S, \hat{\boldsymbol{x}}_S; \boldsymbol{\Phi}_S$ as $\boldsymbol{x}_I, \hat{\boldsymbol{x}}_I; \boldsymbol{\Phi}_I$ restricted on indexing set D and S, respectively. We can judge by intuition from Fig. 1 that, the pseudo-inverse of $\boldsymbol{\Phi}_D$ has significant effect of magnifying noise than that of $\boldsymbol{\Phi}_S$, so it can be predicted the reconstruction error on support set D. The question is, whether this error on D can be transmitted onto S via non-linear processing, thus severely destroy the reconstruction accuracy and stability of the reserved area.

If in the original scene, all targets locate at the region marked by set S, namely area of saving, then the integral problem and the sub-problem is strictly equivalent, thus from formula Eq. (6) we can conclude the reconstruction error follows:

$$\|\boldsymbol{e}_S\|_2 \le C \left\| \left(\boldsymbol{\Phi}_\Lambda^* \boldsymbol{\Phi}_\Lambda\right)^{-1} \boldsymbol{\Phi}_\Lambda^* \boldsymbol{n} \right\|_2 \le C \frac{\|\boldsymbol{n}\|_2}{\sigma_{\min}(\boldsymbol{\Phi}_S)} \quad (9)$$

where, $\|\ \|_2$ denotes 2-norm of a vector, $\sigma_{\min}(\boldsymbol{\Phi}_S)$ denotes the minimum singular value of matrix $\boldsymbol{\Phi}_S$.

If in the original scene, some targets locate at the region marked by set D, namely area of dropping, then the reconstruction error will affect the reconstruction accuracy of area of saving because of the non-linear feature of the method. Under such conditions, specific measurement of the error diffusion phenomenon is required.

From Eq. (6) and the method to get inverse matrix, we can get:

$$\begin{aligned} \boldsymbol{e}_S = \hat{\boldsymbol{x}}_S - \boldsymbol{x}_S = C\left(\boldsymbol{\Phi}_S^* \boldsymbol{P}_{\boldsymbol{\Phi}_D}^{\perp} \boldsymbol{\Phi}_S\right)^{-1} \boldsymbol{\Phi}_S^* \boldsymbol{n} \\ + C\left(\boldsymbol{\Phi}_S^* \boldsymbol{P}_{\boldsymbol{\Phi}_D}^{\perp} \boldsymbol{\Phi}_S\right)^{-1} \boldsymbol{\Phi}_S^* \boldsymbol{P}_{\boldsymbol{\Phi}_D} \boldsymbol{n} \end{aligned} \quad (10)$$

where, $\boldsymbol{P}_{\boldsymbol{\Phi}_D}, \boldsymbol{P}_{\boldsymbol{\Phi}_D}^{\perp}$ is the vector's projection and orthogonal projection to the spaces generated by $\boldsymbol{\Phi}_D$'s columns. Under the premise of reasonable design of sampling and sufficiently sparse of the scene, $\boldsymbol{\Phi}_S$ and $\boldsymbol{\Phi}_D$ still remain approximately orthogonal. Thus in Eq. (10), we can roughly consider $\boldsymbol{P}_{\boldsymbol{\Phi}_D}^{\perp} \boldsymbol{\Phi}_S = \boldsymbol{\Phi}_S$. So we can get from Eq. (10) that:

$$\begin{aligned} \|\boldsymbol{e}_S\|_2 &\le C\left\|\left(\boldsymbol{\Phi}_S^* \boldsymbol{P}_{\boldsymbol{\Phi}_D}^{\perp} \boldsymbol{\Phi}_S\right)^{-1} \boldsymbol{\Phi}_S^* \boldsymbol{n}\right\|_2 \\ &\quad + C\left\|\left(\boldsymbol{\Phi}_S^* \boldsymbol{P}_{\boldsymbol{\Phi}_D}^{\perp} \boldsymbol{\Phi}_S\right)^{-1} \boldsymbol{\Phi}_S^* \boldsymbol{P}_{\boldsymbol{\Phi}_D} \boldsymbol{n}\right\|_2 \\ &\le C\frac{\|\boldsymbol{n}\|_2 + \left\|\boldsymbol{P}_{\boldsymbol{\Phi}_D} \boldsymbol{n}\right\|_2}{\sigma_{\min}(\boldsymbol{\Phi}_S)} \le 2C\frac{\|\boldsymbol{n}\|_2}{\sigma_{\min}(\boldsymbol{\Phi}_S)} \end{aligned} \quad (11)$$

Compare this equation with Eq. (9), we can see the construction error of the area of saving of sub-problem is less than two times of the upper-bound of the overall reconstruction error. So, as the integral problem is divided into sub-problems, the reconstruction error of the sub-problem on area of saving will be affected by the reconstruction error on area of dropping, and tend to enlarge, but has a limit degree.

3.3 Sparse sub-block imaging progress

To sum up the principle discussed above, sparse scene sub-block imaging progress can be described as follows:

Step 1 Block decompose

Denote the time window receiving echo as $[t_1, t_2]$, which is divided into equal-size overlapped sub-intervals $[t_{1,I}, t_{2,I}], I = 1, \cdots, N_b$, each satisfy $t_{2,I} - t_{1,I+1} \ge T$, T is the pulse duration time; based on the sub-blocks $[t_{1,I}, t_{2,I}]$, we can allocate sparse sample as $y[i] = s(t_i), t_i \in [t_{1,I}, t_{2,I}]$, to establish different sparse sample matrix $\boldsymbol{\Theta}_I$; based on the size of the sub-block, we can establish a same radar observation matrix $\boldsymbol{H}_I$, and combine $\boldsymbol{\Theta}_I$ to get the observation sub-matrix $\boldsymbol{\Phi}_I$.

Step 2 Solve sub-problems

By using Lasso to solve sub-problem Eq. (8) in turn, we can get result $\boldsymbol{x}_I$ of the I-th sub-problem; then calculate the corresponding echo time-delay interval $[t_{1,I} - (T/2), t_{2,I} + (T/2)]$, set the result to zero on the area of dropping

$$\tau \in \left[t_{1,I} - \frac{T}{2}, t_{1,I} + \frac{T}{2}\right] \cup \left[t_{2,I} - \frac{T}{2}, t_{2,I} + \frac{T}{2}\right]$$

Step 3 Merge the sub-results

Align the interval of definition $[t_{1,I} - (T/2), t_{2,I} + (T/2)], I = 1, \cdots, N_b$ of each sub-result by time, and superimpose each result by the 'overlapping save' method to get the final result.

4 Numerical and Experimental Results

4.1 Numerical results

In the simulation, assume the radar waveform is chirp, the bandwidth and the duration of which is 150 MHz and 6 μs, respectively. Let the scene be a one dimensional region of length 2700 m, and be decomposed into 2700 uniform range cells. Randomly put some point target into the scene, and sample the echo with an average sampling rate that is 25% of the Nyquist's rate.

Fig. 3 compares the result and error of overall algorithm and sub-block algorithm based on Lasso. In particular, Fig. 3(a) compares the result of the overall algorithm and the sub-block algorithm in noise free case with the original scene, which includes three point targets with different amplitude. It shows that both the overall algorithm and the sub-block algorithm can accurately reconstruct the back-scattered coefficients of the original scene. Define the Relative Mean Square Error (RMSE) as

$$\mathrm{RMSE}(\mathrm{dB}) = 10\lg E\left(\frac{\|\hat{\boldsymbol{x}} - \boldsymbol{x}\|_2^2}{\|\boldsymbol{x}\|_2^2}\right) \quad (12)$$

where, $\boldsymbol{x}, \hat{\boldsymbol{x}}$ is the original and reconstructed back-scattered coefficients. Fig. 3(b) demonstrates the simulated RMSE when the input Signal-to-Noise Ratio (SNR) is chosen as SNR=0 dB, −5 dB, −10 dB, −15 dB, and the number of point targets (k) is chosen as k=11～20. The result shows that the RMSE of sub-block reconstruction is lager than the overall reconstruction, but not more than two times of it.

4.2 Experimental results

The aforementioned sub-block algorithm can generate to azimuth processing and two dimensional imaging of SAR. In the following, the overall and the sub-block algorithm is performed onto the sparse imaging processing of the RadarSat-1 data from the English Bay, Vancouver, Canada[1]. The calculation platform is Intel Core2 3.16 GHz with 4G bytes memory.

The sparse scene is selected from a small region of English Bay, which includes 4 ships located separately. Due to the sparsity characteristic of the scene, the sparse signal processing method can be perform to reconstruct the scene from sub-sampled SAR data. In particular, the number of range sample is preserved and the number of the azimuth sample is 25% of the original data.

Fig. 4(a) demonstrates the overall reconstruct-tion result given by one of the Lasso based algorithm, the Iterative Soft Thresholding Algorithm (ISTA). The total time cost is 45.5 s. Fig. 4(b) demonstrates the result given by sub-block reconstruction also based on ISTA. In sub-block processing, the original scene is divided into 5 uniform sub-regions along the azimuth direction and so as to the SAR data. Each sub-region contains one ship or none and is reconstructed independently. The total time cost is 7.8 s, which 5.8 times smaller than that of the overall reconstruction.

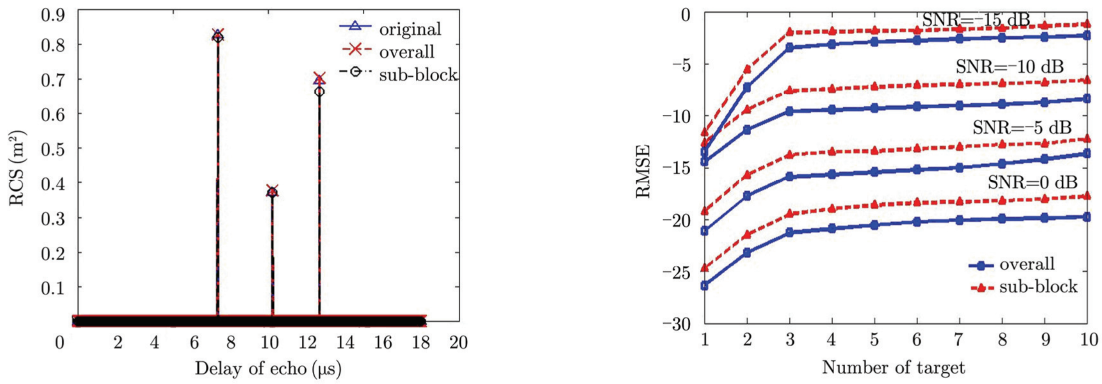

(a) Noise free case

(b) Reconstructed RMSE of sparse scene with different sparsity, input SNR = 0 dB, −5 dB, −10 dB, −15 dB

Fig. 3 Lasso based reconstruction of one dimensional scene, non-uniform sub-sampling, average sampling rate is 25% of the Nyquist's rate

(a) Overall reconstruction

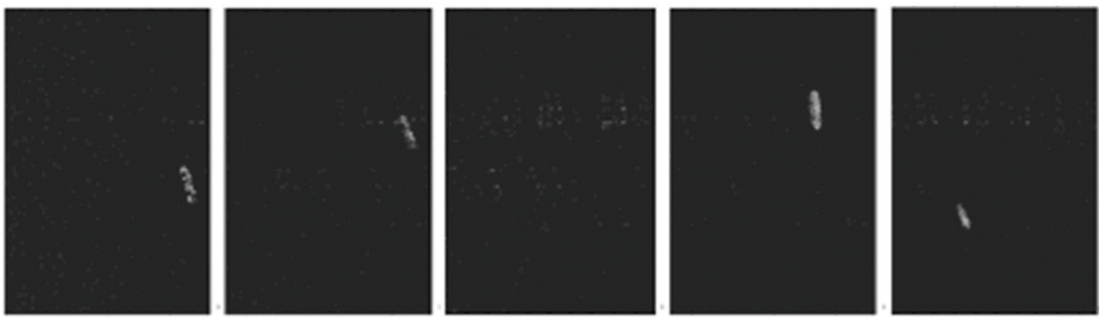

(b) Sub-block reconstruction

Fig. 4 Reconstruction result of a local sparse region of English Bay, Vancouver, Canada from RadarSat1data, 25% sub-sampling along the azimuth

5 Summary

Based on Lasso framework of sparse signal processing, the sub-block algorithm is studied, in which the measured data and the relative imaging region is divided into sub-blocks, and then sparse microwave imaging algorithm based on Lasso is performed on each sub-block, finally the sub-blocks are combined to obtain the whole image of the large scene. The discussed algorithm can greatly improve the computation efficiency to imaging large scene while the reconstruction accuracy would not descend too much.

Reference

[1] Writen by Lan G Cumming, Frank H Wong, translated by Wen Hong, *et al.*. Digital Processing of Synthetic Aperture Radar Date: Algorithms and Implementation[M]. Beijng: Publishing House of Electronics Industry, 2007, Chap. 1.

[2] Wu Yirong, Zhang Bingchen, and Hong Wen. Sparse microwave imaging: principles and applications[J]. *SCIENCE CHINA Information Sciences*, 2012, 55(8): 1722–1754.

[3] Donoho D L. Compressed sensing[J]. *IEEE Transactions on Information Theory*, 2006, 52(4): 1289–1306.

[4] Candès E J and Wakin M B. An introduction to compressive sampling[J]. *IEEE Signal Processing Magazine*, 2008, 25(2): 21–30.

[5] Baraniuk R and Steeghs P. Compressive radar imaging[C]. IEEE Radar Conference, Waltham, Massachusetts, 2007: 128–133.

[6] Patel V M, Easley G R, Healy D M, Jr., *et al.*. Compressed synthetic aperture radar[J]. *IEEE Journal of Selected Topics in Signal Processing: Special Issue on Compressive Sensing*, 2010, 4(2): 244–254.

[7] Fang J, Xu Z B, Zhang B C, *et al.*. Fast compressed sensing SAR imaging based on approximated observation. http://arxiv.org/abs/1302. 3120, Jan. 9, 2013.

[8] Candès E J and Fernandez-Granda C. Towards a mathematical theory of super-resolution. To appear in *Communications on Pure and Applied Mathematics*.

[9] Candès E, Femandez-Granda C. Towards a mathematical theory of super-resolution. http://arxiv.org/abs/1203. 5871, Mar. 27, 2012.

[10] Candès E and Romberg J. Sparsity and incoherence in compressive sampling[J]. *Inverse Problems*, 2007, 23(3): 969–985.

Xiang Yin (1981–), Male, Hubei, China; Ph.D. 2010 in the Institute of Electronics, Chinese Academy of Sciences, Beijing, China; Post-doctor in Institute of Electronics, Chinese Academy of Sciences; Current research activities: compressive sensing, synthetic radar imaging and processing.

E-mail: xy_overlimit@sina.cn

Zhang Bing-chen (1973–), male. He received the B.S. degree in the University of Science and Technology of China (USTC), in 1996, and M.S. degree in the Institute of Electronic, Chinese Academy of Sciences (IECAS), in 1999. He is now the researcher of IECAS and his research interests include radar system and radar signal processing.

E-mail: bczhang@mail.ie.ac.cn

Hong Wen, Scientist in Institute of Electronics, Chinese Academy of Sciences. Ph.D. 1997 from Beijing University of Aeronautics and Astronautics (BUAA), Beijing, China. M.Sc. 1993 from Northwestern Polytechnical University, Xi'an, China. Current research activities: synthetic aperture radar imaging and its applications.

E-mail: grad.mitl@mail.ie.ac.cn